Reconfigurable broadband mode (de)multiplexer based on an integrated thermally induced long-period grating and asymmetric Y-junction

Zhao, Wei Ke; Feng, Jing; Chen, Kai Xin; Chiang, Kin Seng

Published in:
Optics Letters

Published: 01/05/2018

Document Version:
Post-print, also known as Accepted Author Manuscript, Peer-reviewed or Author Final version

Publication record in CityU Scholars:
Go to record

Published version (DOI):
10.1364/OL.43.002082

Publication details:
Zhao, W. K., Feng, J., Chen, K. X., & Chiang, K. S. (2018). Reconfigurable broadband mode (de)multiplexer based on an integrated thermally induced long-period grating and asymmetric *Y*-junction. *Optics Letters*, *43*(9), 2082-2085. Advance online publication. https://doi.org/10.1364/OL.43.002082

Reconfigurable broadband mode (de)multiplexer based on integrated thermally-induced Long-period grating and asymmetric Y-junction

WEI KE ZHAO,[1] JING FENG,[1] KAI XIN CHEN,[1 *] AND KIN SENG CHIANG[2]

[1] School of Optoelectronic Science and Engineering, University of Electronic Science and Technology of China, Chengdu 611731, China
[2]Department of Electronic Engineering, City University of Hong Kong, 83 Tat Chee Avenue, Kowloon, Hong Kong SAR, China
**Corresponding author: chenkx@uestc.edu.cn*

Received XX Month XXXX; revised XX Month, XXXX; accepted XX Month XXXX; posted XX Month XXXX (Doc. ID XXXXX); published XX Month XXXX

We propose a reconfigurable broadband mode (de)multiplexer based on a thermally-induced long-period grating integrated with an asymmetric Y-junction. Any of the two spatial modes of a two-mode waveguide launched into the grating end of the device can be switched into any of the two output ports of the Y-junction by controlling the electric power applied to the electrode heater that induces the grating. Our typical device fabricated with polymer material, which has a length of ~14 mm, shows a mode selectivity higher than 12 dB over the C+L band at a switching power of 198 mW. The device could find applications in reconfigurable mode-division-multiplexing systems.

OCIS codes: (130.3120) Integrated optics devices; (130.4815) Optical switching devices; (130.5460) Polymer waveguides; (050.2770) Gratings; (060.4230) Multiplexing; (060.1810) Buffers, couplers, routers, switches, and multiplexers.

http://dx.doi.org/10.1364/OL.99.099999

Mode (de)multiplexers, which are critical components used for combining or separating different mode channels in mode-division-multiplexing (MDM) optical transmission systems, have received much attention in recent years [1]. Various types of mode (de)multiplexers based on bulk-optic components [2], optical fibers [3, 4], and optical waveguides [5-11] have been proposed. Among these, waveguide-based mode (de)multiplexers have the advantages of compactness, design and fabrication flexibility, fiber compatibility, and integration capability. More importantly, the waveguide technology can offer various material platforms for the incorporation of thermo-optic [12–16] and electro-optic [17–19] effects to realize more powerful mode-controlling devices.

It is envisaged that future MDM networks are reconfigurable and compatible with the existing wavelength-division-multiplexing technology. There is a need to develop reconfigurable mode (de)multiplexers capable of providing spatial switching of mode channels over a wide bandwidth, preferably over the entire C+L band (1530 – 1610 nm). A reconfigurable mode (de)multiplexer can be realized by connecting a fixed mode (de)multiplexer to a spatial optical switch [20] or by integrating a fixed mode (de)multiplexer with a compatible switchable structure [12–17]. Various waveguide structures have been used in integrated reconfigurable mode (de)multiplexers, which include microring resonator [12, 13], symmetric Y-junction [14], directional coupler (DC) [15], Mach-Zehnder interferometer (MZI) [13–17], and multimode interference waveguide (MMI) [17]. Some structures are intrinsically wavelength-sensitive and can only operate over narrow bandwidths [12, 13]. In Ref. 14, the bandwidth for an extinction ratio (ER) higher than 13 dB is only 9 nm, while in Refs. 16 and 17, the bandwidths for an ER higher than 10 dB are 10 nm and 40 nm, respectively. In Ref. 15, a bent DC-assisted MZI is carefully designed to extend the bandwidth to 60 nm (1520 – 1580 nm) for an ER of 12 dB. In this letter, we propose a compact and robust waveguide-based reconfigurable two-mode (de)multiplexer that can operate over the C+L band with an ER (or a mode selectivity) higher than 12 dB.

Our proposed reconfigurable mode (de)multiplexer is formed with a two-mode waveguide connected to an asymmetric Y-junction, where a set of periodic heating electrodes is deposited on the two-mode waveguide. By applying electric power to the electrodes, a long-period grating (LPG) is thermally induced in the waveguide [21], which enables strong conversion between the two spatial modes of the waveguide [22]. As a result, by turning on or off the LPG, the two spatial modes of the waveguide can be selectively directed into the two output ports of the Y-junction. Our LPG mode converter is designed to provide a wide bandwidth by operating it around the turning point along the phase-matching curve of the two modes of the waveguide [23]. The asymmetric Y-junction as a mode splitter can provide an even wider bandwidth [24–27]. We fabricated the device with polymer material by the conventional microfabrication process. With the fundamental mode launched into the device, the mode selectivity measured

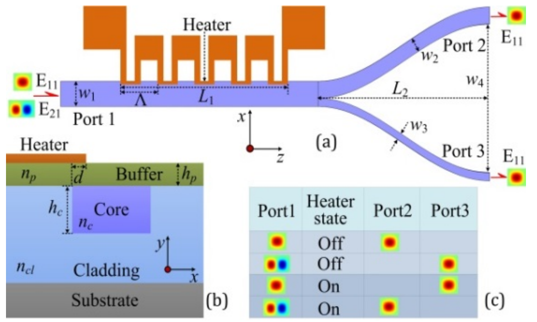

Fig. 1. Schematic diagrams showing (a) the top view and (b) thecross-sectional view of the proposed reconfigurable mode (de)multiplexer, and (c) the switching characteristics of the device as a mode demultiplexer.

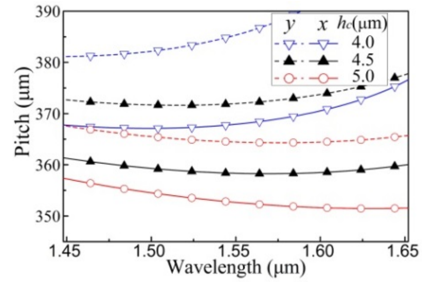

Fig. 2. Phase-matching curves calculated for three different values of the core height h_c (4.0, 4.5 and 5.0 μm) at a fixed core width of w_1 = 8.5 μm.

over the C+L band is larger than 13 dB or 12 dB, with the LPG turned off or on. With the higher-order mode as the input mode, the mode selectivity is 16 dB or 13 dB, also measured with the LPG turned off or on. The maximum switching power required is 198 mW. The total length of the device is ~14 mm and the insertion losses for the two output ports of the Y-junction are 12 dB and 15 dB, respectively, which include fiber-waveguide coupling losses. Compared with previously reported reconfigurable mode multiplexers [12–17], our device has a much simpler structure and offers a wider bandwidth.

Figure 1(a) shows schematically the structure of the proposed mode (de)multiplexer, which consists of an asymmetric Y-junction with periodic heater electrodes deposited on one side of its stem. The heater has pitch Λ and length L_1. The stem of the Y-junction is a straight two-mode waveguide with core width w_1. The core of the two-mode waveguide branches out gradually into two dissimilar single-mode cores with widths w_2 and w_3 ($w_2 > w_3$), respectively, with cosine S-bends extending over a distance L_2 to a maximum separation w_4. All the waveguide cores are of rectangular shape with identical heights h_c. The cross section of the two-mode waveguide is shown in Fig. 1(b). A buffer layer with thickness h_p is used to separate the electrode heater from the core and the heater is placed on one side of the core with an offset distance d. The refractive indices of the core, the cladding, and the buffer are denoted as n_c, n_{cl}, and n_p, respectively. The two-mode waveguide supports the E_{11} and E_{21} modes, each of which has two polarizations, namely the quasi-TE and the quasi-TM polarization – or simply referred to as the x and the y polarization, respectively.

The switching characteristics of the proposed device as a mode demultiplexer are shown in Fig. 1(c). When the heater is off, the E_{11} (E_{21}) mode launched into Port 1 evolves adiabatically into the E_{11} mode in the wide (narrow) arm of the Y-junction and exits from Port 2 (Port 3). When the heater is on, a thermally-induced LPG is generated on one side of the waveguide by the thermo-optic effect. The LPG converts the input E_{11} (E_{21}) mode into the E_{21} (E_{11}) mode, which then evolves into the E_{11} mode in the narrow (wide) arm of the Y-junction and exits from Port 3 (Port 2). The device can function as a mode multiplexer by operating it in the reverse direction, i.e., light launched into Port 2 or Port 3 can be switched between the E_{11} and E_{21} modes at Port 1.

In our study, we use the UV-curable polymer materials EpoCore and EpoClad (Micro Resist Technology) as the core and the cladding material, respectively, and PMMA as the buffer material. The refractive indices of these materials, measured with a commercial prism coupler (Metricon 2010) on thin-film samples at 1538 nm, are n_c = 1.5716 (1.5709) for the x (y) polarization, n_{cl} = 1.5595, and n_p = 1.4793 for both polarizations. With these material parameters, we design the two-mode waveguide by solving the modes with a commercial mode solver (COMSOL), assuming a buffer thickness of h_p = 1.5 μm and a thick cladding layer. We fix the core width at w_1 = 8.5 μm and study the effect of the core height h_c on the grating pitch Λ, which is given by the phase-matching condition $\Lambda = \lambda_0/(N_{11} - N_{21})$, where N_{11} and N_{21} are the effective indices of the E_{11} and E_{21} modes, respectively, and λ_0 is the resonance wavelength. Figure 2 shows the dependence of the resonance wavelength on the grating pitch, calculated for three core heights: h_c = 4.0, 4.5, and 5.0 μm. Because of the geometry and the material birefringence, the phase-matching curves for the two polarizations are different. In this study, we design the device to ensure desirable operation for the x polarization. As shown in Fig. 2, the phase-matching curves are quite flat, which suggests the possibility of broadband operation for a given grating pitch. For our design, we choose h_c = 4.5 μm and a grating pitch of Λ = 358 μm, which corresponds to the turning point of the phase-matching curve at 1575 nm. With these parameters, the LPG should operate over the C+L band. The electrode heater has a width of 30 μm, a duty cycle of 48%, a length of L_1 = 5744 μm, and an offset distance of d = 1.0 μm from the edge of the core. We determine the heater position by analyzing the dependence of the temperature distribution on the heater position for optimizing the grating effect (calculated with COMSOL at an ambient temperature of 20 °C). We also confirm that the thermally-induced bulk-index change has negligible effects on the mode-field distributions. To design the device for the y polarization, we may keep h_c = 4.5 μm and increase the grating pitch to Λ = 373 μm, as shown in Fig. 2.

Given the parameters of the two-mode waveguide (w_1 = 8.5 μm and h_c = 4.5 μm), the parameters of the Y-junction branches are determined with a 3D finite-difference beam propagation method (3DFD-BPM) (BeamPROP, RSoft) by optimizing the mode selectivity of the Y-junction. Here the mode selectivity is defined as $R = |10\log(P_2/P_3)|$, where P_2 and P_3 are the output powers from Port 2 and Port 3, respectively, when the E_{11} mode or the E_{21} mode is launched into Port 1. Our extensive numerical analysis shows that a polarization-independent mode selectivity larger than 29 dB (with either mode as the input mode) can be achieved over the wavelength range 1400 – 1700 nm with w_2 = 5.7 μm, w_3 = 2.8 μm, w_4 = 127 μm, and L_2 = 6300 μm. These are the parameters used in our final design.

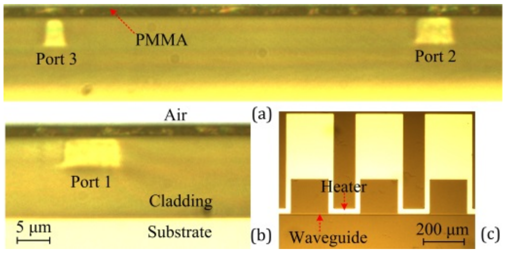

Fig. 3. Microscope images of (a) the demultiplexing end, (b) the multiplexing end, and (c) the periodic heater electrodes of the fabricated device.

We fabricated the proposed device with the design parameters given earlier by the standard photolithography process. An EpoClad film was first spin-coated onto an oxidized Si substrate to a thickness of ~8.0 µm to form the lower cladding. An EpoCore film was next spin-coated onto the lower cladding to a thickness of 4.5 µm to form the core layer, which was then chemically etched into the pattern of the device by the photolithography process. Subsequently, an Epoclad film was spin-coated onto the core to form the side claddings, where the spin-coating speed was carefully controlled to minimize excess covering of Epoclad on the core. After the EpoClad layer was cured, a PMMA film was spin-coated onto the waveguide to a thickness of ~1.5 µm to form the buffer layer. Finally, a 150-nm thick Cr layer and a 400-nm thick Al layer were successively deposited onto the PMMA layer by RF sputtering and thermal evaporation and periodic heater electrodes were formed by applying photolithography and chemical etching to the metal layers. The total length of the device was 14 mm. Microscope images of the two end faces of the fabricated device and the periodic heater electrodes are shown in Fig. 3.

We first characterized the performance of the fabricated device as a mode multiplexer. Light from a tunable laser (Santur TL-2020-C-107) was made to pass through a polarization controller (PC) and then launched into Port 2 or Port 3 to excite the E_{11} mode with a lensed single-mode fiber (SMF). The near-field images taken at Port 1 with an infrared camera (MicronViewer 7290A) when the heater was off are shown in Fig. 4(a). Over the wavelength range 1530 – 1560 nm available with the laser source, the E_{11} mode launched into Port 2 (Port 3) evolves into the E_{11} (E_{21}) mode at Port 1 with weak polarization dependence, which agrees with the expected operation of the Y-junction. We next replaced the tunable laser with a (C+L)-band amplified spontaneous emission (ASE) source (B&A Technology AS4600) and observed how the mode patterns at Port 1 varied with the applied heater power. The results are shown in Fig. 4(b). With the heater turned off, the output near-field images are similar to those measured with the tunable laser, which confirms the broadband operation of the Y-junction. As shown in Fig. 4(b), the output near-field images change with the applied heater power. For the *x*-polarized light launched into Port 2 (Port 3), at a heater power of 198 mW, the E_{11} (E_{21}) mode at Port 1 is almost completely switched to the E_{21} (E_{11}) mode. These results confirm broadband operation of the device as a mode multiplexer. The device does not work well for the *y* polarization, which is expected, as the LPG is optimized only for the *x* polarization.

We next characterized the performance of the fabricated device as a mode demultiplexer by launching the *x*-polarized E_{11} and E_{21} modes, respectively, into Port 1 with the ASE source. To excite the

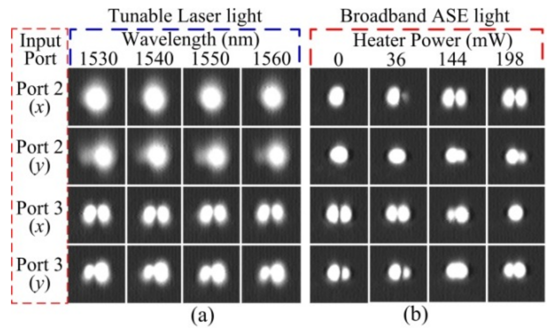

Fig. 4. Near-field images taken at Port 1 of the fabricated device (a) when the *x*- or *y*-polarized light from a tunable laser source was launched into Port 2 or Port 3 with the heater turned off, and (b) when *x*- or *y*-polarized light form a (C+L)-band ASE source was launched into Port 2 or Port 3 with different electric powers applied to the heater.

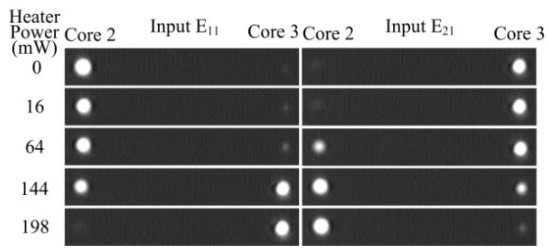

Fig. 5. Near-field images taken at Port 2 and Port 3 for different heater powers, when the *x*-polarized E_{11} (a) and E_{21} (b) modes were launched into Port 1, respectively.

E_{21} mode at Port 1, we adjusted the lensed SMF carefully to introduce a suitable offset from the center of the core and a small tilt angle from the core axis. Figure 5 shows the near-field images taken at Port 2 and Port 3 for different heater powers. As the device does not work well for the *y* polarization, the results for the *y* polarization are not shown. As shown in Fig. 5, the highest mode selectivity is achieved at a switching power of 198 mW. The mode selectivity of the device is limited by several factors: the purity of the excited mode at Port 1, imperfect function of the Y-junction, and any stress induced by the deposition of the metal electrodes on the waveguide [21].

We also measured the transmission spectra of the device by connecting Port 2 and Port 3, respectively, to an optical spectrum analyzer (Anritsu MS9740A) via an SMF. Figure 6 shows the normalized transmission spectra of Port 2 and Port 3, measured with the *x*-polarized E_{11} and E_{21} modes launched, respectively, into Port 1, for both the "off" (0 heater power) and "on" (198-mW heater power) states. Over the C+L band, with the heater turned off, the mode selectivity of the device is between 13 – 21 dB for the E_{11} mode input and 16 – 25 dB for the E_{21} mode input, while, with the heater turned on, the mode selectivity is 12 – 23 dB for the E_{11} mode input and 13 – 23 dB for the E_{21} mode input.

We measured the insertion losses of the device at 1550 nm by launching *x*-polarized light into Port 2 and Port 3 with an SMF, respectively, and measuring the corresponding output power from Port 1 with a power meter. The losses are 12 dB for Port 2 and 15 dB for Port 3, which include fiber-waveguide coupling losses at the

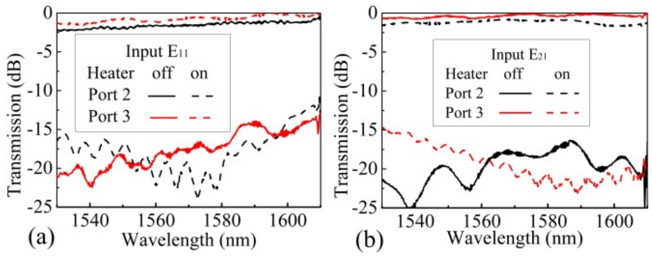

Fig. 6. Normalized transmission spectra of Port 2 and Port 3 measured for the "off" and "on" states of the heater with the *x*-polarized (a) E_{11} and (b) E_{21} modes launched, respectively, into Port 1.

two ends. The propagation losses of the E_{11} mode, measured by the cut-back method at 1550 nm, are 2.8, 3.5, and 4.8 dB/cm for the stem, the wide arm, and the narrow arm of the Y-junction, respectively, while the propagation loss of the E_{21} mode for the stem is about 4 dB/cm.

The relatively large insertion losses of the device are partly due to the polymer material system used in our work, which is developed mainly for applications at 850 nm at which the loss is <0.2 dB/cm. Its absorption loss in the C band is 1 – 2 dB/cm. Regardless of its relatively large loss in the C band, this material system has been used successfully for demonstrating various novel device designs [7, 9, 22, 26]. The other source of loss is the scattering loss caused by the roughness and inhomogeneity along the waveguides introduced in the fabrication process, which depends on the skill of the fabricator, the ambient, and the facilities. There should be much room to reduce the losses of our device by improving the fabrication skill and using a low-loss polymer material system [28]. The device could also be implemented with other material systems, such as SiN and Si, to reduce the footprint and the power consumption.

In conclusion, we have proposed and fabricated a reconfigurable broadband mode (de)multiplexer for the E_{11} and E_{21} modes of a two-mode waveguide by integrating a thermally-induced LPG and an asymmetric Y-junction. Our device combines the merits of effective mode conversion with an LPG and broadband mode selectivity with an asymmetric Y-junction. We have designed the LPG carefully to provide broadband mode conversion, so that the whole device can operate over the entire C+L band. Our typical fabricated device, which has a length of 14 mm, shows a mode selectivity larger than 12 dB over the C+L band for the quasi-TE polarization at a switching power of 198 mW. It should be possible to extend our device architecture to handle more spatial modes by employing a multi-arm Y-junction with a multimode stem [25] or a three-dimensional asymmetric waveguide branch [26], or by cascading a series of devices designed for different modes [27]. Few-mode waveguide devices, such as the one demonstrated in this study, can be butt-coupled to few-mode circular-core and elliptical-core fibers with little modal crosstalks, when the waveguide cores are properly shaped to match the core dimensions of the fibers [29]. Our device could find applications in reconfigurable MDM systems based on circular-core or elliptical-core fibers [30].

Funding. National Natural Science Foundation of China (NSFC) (61377057); Open Fund of IPOC of BUPT (Project IPOC2016B007); the State Key Laboratory of Integrated Optoelectronics at Jilin University, China (Project IOSKL2016KF10); Research Grants Council, University Grants Committee, Hong Kong (CityU 11253316).

References

1. G. F. Li, N. Bai, N. B. Zhao, and C. Xia, Adv. Opt. Photon. **6**, 413 (2014).
2. G. Labroille, B. Denolle, P. Jian, P. Genevaux, N. Treps, and J.-F. Morizur, Opt. Express **22**, 15599 (2014).
3. S. H. Chang, H. S. Chung, N. K. Fontaine, R. Ryf, K. J. Park, K. Kim, J. C. Lee, J. H. Lee, B. Y. Kim, and Y. K. Kim, Opt. Express **22**, 14229 (2014).
4. A. M. Velazquez-Benitez, J. C. Alvarado, G. Lopez-Galmiche, J. E. Antonio-Lopez, J. Hernández-Cordero, J. Sanchez-Mondragon, P. Sillard, C. M. Okonkwo, and R. Amezcua-Correa, Opt. Lett. **40**, 1663 (2015).
5. J. Wang, S. L. He, and D. X. Dai, Laser Photon. Rev. **8**, L18 (2014).
6. K. Saitoh, N. Hanzawa, T. Sakamoto, T. Fujisawa, Y. Yamashita, T. Matsui, K. Tsujikawa, and K. Nakajima, Opt. Fiber Technol. **35**, 80 (2017).
7. J. Dong, K. S. Chiang, and W. Jin, Opt. Lett. **40**, 3125 (2015).
8. Y. Wu and K. S. Chiang, Opt. Lett. **42**, 407 (2017).
9. W. K. Zhao, K. X. Chen, J. Y. Wu, and K. S. Chiang, IEEE Photon. J. **9**, Art no. 6601509 (2017).
10. J. M. Baumann, E. P. D. Silva, Y. H. Ding, K. Dalgaard, L. H. Frandsen, L. K. Oxenlowe, and T. Morioka, in *Optical Fiber Communication Conference,* San Diego, Calif. (Optical Society of America, 2018), paper W1E.4.
11. O. M. Nawwar, H. M. H. Shalaby and R. K. Pokaharel, Appl. Opt. **57**, 42 (2018).
12. B. Stern, X. L. Zhu, C. P. Chen, L. D. Tzuang, J. Cardenas, K. Bergman, and M. Lipson, Optica **2**, 530 (2015).
13. C. L. Sun, Y. Yu, G. Y. Chen, and X. L. Zhang, Opt. Lett. **41**, 3257 (2016).
14. W. Y. Chan and H. P. Chan, Opt. Express **22**, 9282 (2014).
15. S. P. Wang, H. Wu, H. K. Tsang, and D. X. Dai, Opt. Lett. **41**, 5298 (2016).
16. D. Melati, A. Alippi, and A. Melloni, Opt. Express **24**, 12625 (2016).
17. Y. L. Xiong, R. B. Priti, and O. L. Ladouceur, Optica **4**, 1098 (2017).
18. M. R. Zhang, K. X. Chen, W. Jin, and K. S. Chiang, Appl. Opt. **55**, 4418 (2016).
19. W. Jin and K. S. Chiang, Opt. Lett. **40**, 237 (2015).
20. N. P. Diamantopoulos, M. Hayashi, Y. Yoshida, A. Maruta, R. Maruyama, N. Kuwaki, K. Takenage, H. Uemura, S. Matsuo, and K. Kitayama, Opt. Express **23**, 23660 (2015).
21. K. S. Chiang, C. K. Chow, Q. Liu, H. P. Chan, and K. P. Lor, IEEE Photon. Technol. Lett. **18**, 1109 (2006).
22. Y. Yang, K. X. Chen, W. Jin, and K. S. Chiang, IEEE Photon. Technol. Lett. **27**, 1985 (2015).
23. S. Ramachandran, Z. Y. Wang, and M. Yan, Opt. Lett. **27**, 698 (2002).
24. J. D. Love and N. Riesen, J. Lightw. Technol. **30**, 304 (2012).
25. N. Riesen and J. D. Love, Appl. Opt. **51**, 2778 (2012).
26. Y. Wu and K. S. Chiang, Opt. Lett. **42**, 407 (2017).
27. W. W. Chen, P. J. Wang, T. J. Yang, G. C. Wang, T. G. Dai, Y. W. Zhang, L. Q. Zhou, X. Q. Jiang, and J. Y. Yang, Opt. Lett. **41**, 2851 (2016).
28. D. D. Felipe, M. Kleinert, C. Zawadzki, A. Polatynski, G. Irmscher, W. Brinker, M. Moehrle, H. Bach, N. Keil and M. Schell, J. Lightw. Technol. **35**, 683 (2017).
29. Y. Wu and K. S. Chiang, Opt. Express **24**, 30108 (2016).
30. N. Riesen, J. D. Love, and J. W. Arkwright, IEEE Photon. Technol. Lett. **24**, 344 (2012).

Full References

1. G. F. Li, N. Bai, N. B. Zhao, and C. Xia, "Space-division multiplexing: the next frontier in optical communication," Adv. Opt. Photon. **6**, 413-487 (2014).
2. G. Labroille, B. Denolle, P. Jian, P. Genevaux, N. Treps, and J.-F. Morizur, "Efficient and mode selective spatial mode multiplexer based on multi-plane light conversion," Opt. Express **22**(13), 15599-15607 (2014).
3. S. H. Chang, H. S. Chung, N. K. Fontaine, R. Ryf, K. J. Park, K. Kim, J. C. Lee, J. H. Lee, B. Y. Kim, and Y. K. Kim, "Mode division multiplexed optical transmission enabled by all-fiber mode multiplexer," Opt. Express **22**(12), 14229-14236 (2014).
4. A. M. Velazquez-Benitez, J. C. Alvarado, G. Lopez-Galmiche, J. E. Antonio-Lopez, J. Hernández-Cordero, J. Sanchez-Mondragon, P. Sillard, C. M. Okonkwo, and R. Amezcua-Correa, "Six mode selective fiber optic spatial multiplexer," Opt. Lett. **40**(8), 1663-1666 (2015).
5. J. Wang, S. L. He, and D. X. Dai, "On-chip silicon 8-channel hybrid (de)multiplexer enabling simultaneous mode- and polarization-divisionmultiplexing," Laser Photon. Rev. **8**(2), L18-L22 (2014).
6. K. Saitoh, N. Hanzawa, T. Sakamoto, T. Fujisawa, Y. Yamashita, T. Matsui, K. Tsujikawa, and K. Nakajima, "PLC-based mode multi/demultiplexers for mode division multiplexing," Opt. Fiber Technol. **35**, 80-92 (2017).
7. J. Dong, K. S. Chiang, and W. Jin, "Mode multiplexer based on integrated horizontal and vertical polymer waveguide couplers," Opt. Lett. **40**(13), 3125-3128 (2015).
8. Y. Wu and K. S. Chiang, "Ultra-broadband mode multiplexers based on three-dimensional asymmetric waveguide branches," Opt. Lett. **42**(3), 407-410 (2017).
9. W. K. Zhao, K. X. Chen, J. Y. Wu, and K. S. Chiang, "Horizontal Directional Coupler Formed With Waveguides of Different Heights for Mode-Division Multiplexing," IEEE Photon. J. **9**(5), Art no. 6601509 (2017).
10. J. M. Baumann, E. P. D. Silva, Y. H. Ding, K. Dalgaard, L. H. Frandsen, L. K. Oxenlowe, and T. Morioka, "Silicon Chip-to-Chip Mode-Division Multiplexing," in *Optical Fiber Communication Conference,* San Diego, Calif. (Optical Society of America, 2018), paper W1E.4.
11. O. M. Nawwar, H. M. H. Shalaby, and R. K. Pokaharel, "Modeling, simulation, and fabrication of bi-directional mode-division multiplexing for silicon-on-insulator platform," Appl. Opt. **57**(1), 42-51 (2018).
12. B. Stern, X. L. Zhu, C. P. Chen, L. D. Tzuang, J. Cardenas, K. Bergman, and M. Lipson, "On-chip mode-division multiplexing switch," Optica **2**(6), 530-535 (2015).
13. C. L. Sun, Y. Yu, G. Y. Chen, and X. L. Zhang, "Integrated switchable mode exchange for reconfigurable mode-multiplexing optical networks," Opt. Lett. **41**(14), 3257-3260 (2016).
14. W. Y. Chan and H. P. Chan, "Reconfigurable two-mode mux/demux device," Opt. Express **22**(8), 9282-9290 (2014).
15. S. P. Wang, H. Wu, H. K. Tsang, and D. X. Dai, "Monolithically integrated reconfigurable add-drop multiplexer for mode-division-multiplexing systems," Opt. Lett. **41**(22), 5298-5301 (2016).
16. D. Melati, A. Alippi, and A. Melloni, "Reconfigurable photonic integrated mode (de)multiplexer for SDM fiber transmission," Opt. Express **24**(12), 12625-12634 (2016).
17. Y. L. Xiong, R. B. Priti, and O. L. Ladouceur, "High-speed two-mode switch for mode-division multiplexing optical networks," Optica **4**(9), 1098-1102 (2017).
18. M. R. Zhang, K. X. Chen, W. Jin, and K. S. Chiang, "Electro-optic mode switch based on lithium-niobate Mach-Zehnder interferometer," Appl. Opt. **55**(16), 4418-4422 (2016).
19. W. Jin and K. S. Chiang, "Mode switch based on electro-optic long-period waveguide grating in lithium niobate," Opt. Lett. **40**(2), 237-240 (2015).
20. N. P. Diamantopoulos, M. Hayashi, Y. Yoshida, A. Maruta, R. Maruyama, N. Kuwaki, K. Takenage, H. Uemura, S. Matsuo, and K. Kitayama, "Mode-selective optical packet switching in mode-division multiplexing networks," Opt. Express **23**(18), 23660-23666 (2015).
21. K. S. Chiang, C. K. Chow, Q. Liu, H. P. Chan, and K. P. Lor, "Band-rejection filter with widely tunable center wavelength and contrast using metal long-period grating on polymer waveguide," IEEE Photon. Technol. Lett. **18**(9), 1109-1111 (2006).
22. Y. Yang, K. X. Chen, W. Jin, and K. S. Chiang, "Widely Wavelength-Tunable Mode Converter Based on Polymer Waveguide Grating," IEEE Photon. Technol. Lett. **27**(18), 1985-1988 (2015).
23. S. Ramachandran, Z. Y. Wang, and M. Yan, "Bandwidth control of long-period grating-based mode converters in few-mode fibers," Opt. Lett. **27**(9), 698-700 (2002)
24. J. D. Love and N. Riesen, "Single-, Few-, and Multimode Y-Junctions," J. Lightw. Technol. **30**(3), 304-309 (2012).
25. N. Riesen and J. D. Love, "Design of mode-sorting asymmetric Y-junctions," Appl. Opt. **51** (15), 2778-2783 (2012).
26. Y. Wu and K. S. Chiang, "Ultra-broadband mode multiplexers based on three-dimensional asymmetric waveguide branches," Opt. Lett. **42**(3), 407-410 (2017).
27. W. W. Chen, P. J. Wang, T. J. Yang, G. C. Wang, T. G. Dai, Y. W. Zhang, L. Q. Zhou, X. Q. Jiang, and J. Y. Yang, "Silicon three-mode (de)multiplexer based on cascaded asymmetric Y junctions," Opt. Lett. **41**(12), 2851-2854 (2016).
28. D. D. Felipe, M. Kleinert, C. Zawadzki, A. Polatynski, G. Irmscher, W. Brinker, M. Moehrle, H. Bach, N. Keil and M. Schell, "Recent developments in polymer based photonic components for Disruptive Capacity Upgrade in Data Centers," J. Lightw. Technol. **35**(4), 683-689 (2017).
29. Y. Wu and K. S. Chiang, "Mode-selective coupling between few-mode fibers and buried channel waveguides," Opt. Express **24** (26), 30108-30123 (2016).
30. N. Riesen, J. D. Love, and J. W. Arkwright, "Few-mode elliptical-core fiber data transmission," IEEE Photon. Technol. Lett. **24**(5), 344-346 (2012).